INHOMOGENEITY OF TISSUE STRAIN DISTRIBUTIONS IN NORMAL AND OSTEOPOROTIC INDIVIDUAL TRABECULAE: MATHEMATICAL MODEL STUDIES

Idit Diamant, Sigal Portnoy, Amit Gefen

Department of Biomedical Engineering
Faculty of Engineering
Tel Aviv University
Tel Aviv 69978, Israel

INTRODUCTION

The traditional interpretation of Wolff law is that mass distribution and microstructural arrangement of trabeculae in cancellous bone are determined by the local mechanical stresses transferred to the bone. According to this interpretation, trabeculae are arranged on paths of equal ("iso") stress, called isostatics. This suggests that along each individual trabecular path, strains should be approximately uniform. Moreover, strains are expected to be rather uniform across different paths since in healthy bones under physiological loads, paths do not spontaneously resorb or break, likely because they are subjected to a narrow range of stresses/strains [1]. However, recent micro- finite element (micro-FE) studies of femoral cancellous bone by van Rietbergen et al. show considerable variation in tissue strains for the external loads acting on the femoral head during the stance phase of gait [1]. Strain magnitudes in an osteoporotic femoral head analyzed by micro-FE in the same study were ~70% higher and less uniformly distributed than those in the healthy femur [1]. These results lead to a subsequent research question: is the inhomogeneity of tissue strains predominantly a consequence of structural differences between trabeculae (inter-trabecula strain variability), or is it caused by the curvatures of each individual trabecula (intra-trabecula strain variability)? Accordingly, the objectives of this study were to determine the contribution of the shape of a trabecula to the intra-trabecula strain inhomogeneity, and to determine differences in intra-trabecula strain inhomogeneities between normal and thinner, osteoporotic-like trabeculae.

METHOD

In order to analytically study strain inhomogeneities in individual trabeculae, we employed our single-trabecula generic 'building block' [2]. Briefly, the generic trabecula 'building block' is an idealization of the geometry of trabeculae (Fig. 1) based on statistical analyses of dimensions of 200 trabeculae, which led to the profile shape of

$$r(z) = \pm \frac{2 \cdot Tb.Th - \beta}{1+\alpha} \left\{ \cos\left(2z/L \ \cos^{-1}\left(1/2 \left(3 - \alpha - \frac{\beta \cdot (1+\alpha)}{2 \cdot Tb.Th - \beta} \right) \right) \right) - 3/2 \right\} \qquad (1)$$

where $r(z)$ is the radius of the trabecula at location z along its length, $Tb.Th$ is the mean thickness of the trabecula across its length (L) and the constants are α=1.3736 and β=40.9 μm [2]. Empirically, we showed that the thickness at the edges of a trabecula $t_{base}=r(z=L/2)$ is proportional to the minimal thickness at the center of a trabecula $t_{center}=r(z=0)$ [2]. One quantitative measure for the inhomogeneity of strains in a trabecula is the difference $\Delta\varepsilon$ between the maximal strain ε_{max} and minimal strain $\varepsilon_{\min}$ along the axis of the trabecula. Assuming small strain elasticity and pure axial compressive force F acting on the edges of a trabecula with an elastic modulus E:

$$\Delta\varepsilon = \frac{F}{E}\left(\frac{1}{A_{\min}} - \frac{1}{A_{\max}} \right) \qquad (2)$$

For an idealized trabecula with a profile shape as in Eq. (1):

$$\Delta\varepsilon = \frac{F}{E}\left(\frac{1}{A_{center}} - \frac{1}{A_{base}} \right) = \frac{4}{\pi}\frac{F}{E}\left(\frac{1}{t_{center}^2} - \frac{1}{t_{base}^2} \right) \qquad (3)$$

Considering the measured constant proportion η between base and center thicknesses [2], $t_{base} = \eta t_{center}$, equation (3) becomes:

$$\Delta\varepsilon = \frac{4F}{\pi E t_{center}^2}\left(1 - \frac{1}{\eta^2} \right) \qquad (4)$$

Now considering two different trabeculae with center thicknesses $t_{center1}$ and $t_{center2}$ and strain inhomogeneities $\Delta\varepsilon_1$ and $\Delta\varepsilon_2$, respectively, and also assuming that $t_{center1}<t_{center2}$ and that both trabeculae have the same modulus E and are subjected to the same load F, Eq. (5) reveals that

$$\Delta\varepsilon_2 / \Delta\varepsilon_1 = \left(t_{center1} / t_{center2} \right)^2 \qquad (5)$$

i.e. the strain inhomogeneity in the thinner trabecula ($\Delta\varepsilon_1$) must be greater than the strain inhomogeneity in the thicker trabecula ($\Delta\varepsilon_2$).

In order to systematically study strain inhomogeneities in trabeculae with different profiles (Eq. 1) subjected to more complex, compound loading (compression + shear + bending) we developed a FE solver (Visual C++ 6, Microsoft Co.) which approximated the profile shape of Eq. (1) using 200 cylindrical elements with varying thicknesses along the z-axis of the trabecula. The elastic modulus of bone tissue was set to E=10 GPa in both normal and osteoporotic simulations [1,2]. We analyzed strain inhomogeneities in trabeculae with dimensions that are characteristic of

cancellous bone in the spine. In a first set of simulations we studied strain distributions and strain inhomogeneities in individual trabeculae. Specifically, we considered normal trabeculae in the spine with Tb.Th of 180 μm and length of 1200 μm, osteoporotic spine trabeculae with Tb.Th of 120 μm and length of 2000 μm, and intermediate Tb.Th/length cases [3,4]. These trabeculae were subjected to identical loads - uniaxial compression force of 0.01N and bending moment of 10^{-6} Nm - a combination which produced small strains (less than 5%) in all simulation cases. In a second set of simulations we studied strain inhomogeneities in statistical "populations" of trabeculae containing trabeculae with different Tb.Th but having the same length (1100 μm, [4]). Specifically, we used Tb.Th in the range of 130-380 μm (mean 180 μm) to represent normal vertebral cancellous bone, and Tb.Th in the range of 60-240 μm (mean 120 μm) to represent osteoporotic vertebral cancellous bone (Fig. 1) [3,4]. Thickness distributions in normal and osteoporotic "populations" of trabeculae were set to be right-skewed (Fig. 2), as reported in experimental studies [2,5]. All trabeculae in a "population" were again subjected to identical compressive and bending loads, of 0.1N and $5*10^{-5}$ Nm, respectively, and it was verified that these loads resulted small deformations (>5%) in all trabeculae.

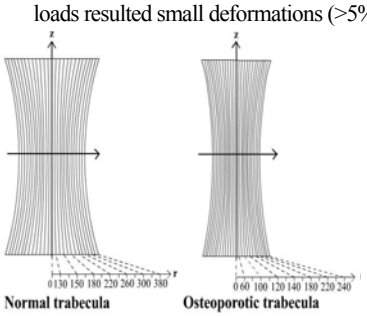

Figure 1. Profile shapes of normal and osteoporotic trabeculae. Thickness is in μm.

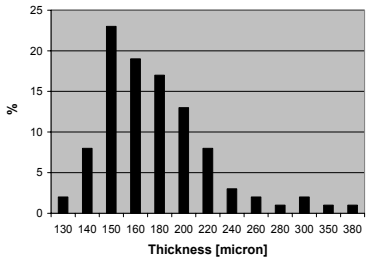

Figure 2. Distribution of thicknesses in a "population" of normal trabeculae.

RESULTS

Consistently with the conclusion derived from Eq. 5, the results for compound loading (compression + bending) demonstrate that as trabeculae become thinner with the progression of osteoporosis, the strain inhomogeneity becomes wider as strain peaks grow higher. Figure 3 shows strain distributions in progressively thinning individual trabeculae. The strain inhomogeneity in the longest (2000 μm) and thinnest (120 μm) trabecula ($\Delta\varepsilon$=~1.4%) is nearly 5-fold that in the shortest (1200 μm) and thickest (180 μm) trabecula ($\Delta\varepsilon$=~0.3%).

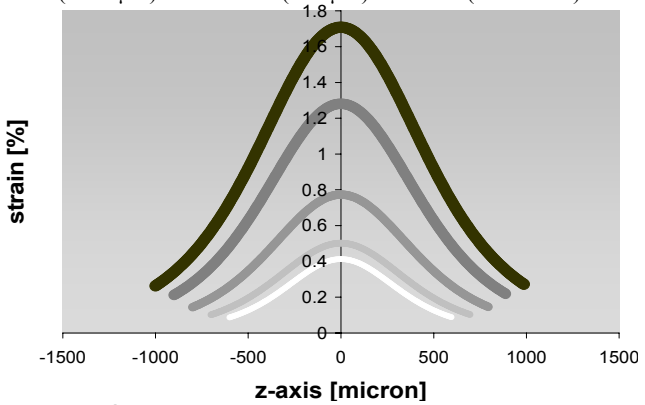

Figure 2. Strain distributions along normal (white line, Tb.Th=180 μm, *L*=1200 μm) and osteoporotic (black line, Tb.Th=120 μm, *L*=2000 μm) trabeculae. Strain distributions for intermediate Tb.Th and lengths are shown in grayscale.

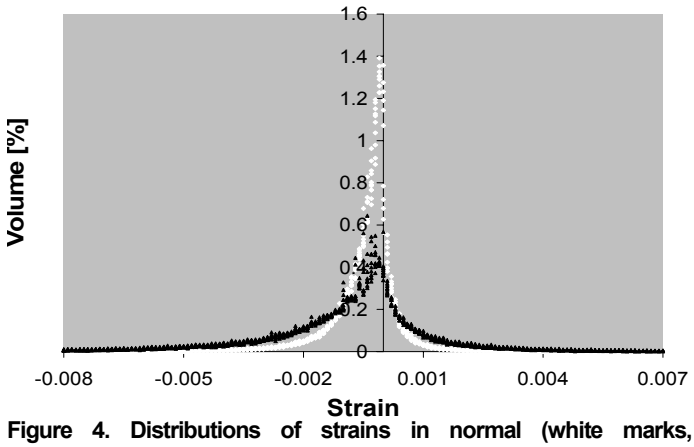

Figure 4. Distributions of strains in normal (white marks, Tb.Th=130-380 μm) and osteoporotic (black marks, Tb.Th=60-240 μm) "populations" of trabeculae. Length of all trabeculae is 1.1 mm.

Figure 4 shows the volumetric distribution of strains across "populations" of normal trabeculae (Tb.Th=130-380 μm, length=1100 μm) and osteoporotic trabeculae (Tb.Th=60-240 μm, length=1100 μm). Consistently with the results for intra-trabecula strain inhomogeneities (Fig. 3), the results for populations show that in normal cancellous bone strains are more uniform than in osteoporotic bone. For the thickness distributions in these simulations, strain inhomogeneity in the osteoporotic cancellous bone ($\Delta\varepsilon$=1.7±1.4%) was more than 3-fold that in the normal cancellous bone ($\Delta\varepsilon$=0.53±0.21%).

DISCUSSION

Our mathematical modeling supports the hypothesis that when subjected to equivalent loads, thinner, osteoporotic-like trabeculae are found under substantially greater strain inhomogeneities compared with normal trabeculae. The results agree with the studies of van Rietbergen et al. [1] and further indicate that intra-trabecula strain inhomogeneities may be a primary factor contributing to the effective strain inhomogeneities observed in their studies of femoral heads [1]. One important assumption in the present analyses is that osteoporotic bones are loaded as normal bones, but in real-life situations, osteoporotic patients may be less active and this may be a compensating effect which reduces strain inhomogeneities in their cancellous bone. Additional micro-FE studies will now be required to distinguish between the contributions of intra-trabecula and inter-trabecula strain inhomogeneities to the overall reported increase in strain inhomogeneity with osteoporosis [1].

REFFERENCES

1. Van Rietbergen B., Huiskes R., Eckstein F., Ruegsegger P. 2003, "Trabecular bone tissue strains in the healthy and osteoporotic human femur," J. Bone Mineral Res., Vol. 18, pp. 1781-1788.
2. Dagan, D., Be'ery, M., Gefen, A. 2004, "Single-trabecula building block for large-scale finite element models of cancellous bone," Med. Biol. Eng. Comput., Vol. 42, pp. 549-556.
3. Werner H. J., Martin H., Behrend D., Schmitz K.P., Schoherf H.C. 1996, "The loss of stiffness as osteoporosis progresses," Med. Eng. Phys., Vol. 18, pp. 601-606.
4. Majumdar, S., Kothari, M., Augat, P., Newitt, D.C., Link, T.M., Lin, J.C., Lang, T., Lu, Y., Genant, H.K. 1998, "High-resolution magnetic resonance imaging: three-dimensional trabecular bone architecture and biomechanical properties," Bone, Vol. 22, pp. 445-54.
5. Kothari, M., Keaveny, T.M., Lin, J.C., Newitt, D.C., Majumdar S. 1999, "Measurement of intraspecimen variations in vertebral cancellous bone architecture," Bone, Vol. 25, pp. 245-50.